DEUTSCHES ELEKTRONEN-SYNCHROTRON DESY

DESY 78/46
September 1978

JETS FROM $Q\bar{Q}$ P WAVES

by

Hartmut Krasemann

NOTKESTRASSE 85 · 2 HAMBURG 52

To be sure that your preprints are promptly included in the
HIGH ENERGY PHYSICS INDEX ,
send them to the following address (if possible by air mail) :

DESY
Bibliothek
Notkestrasse 85
2 Hamburg 52
Germany

Jets from $Q\bar{Q}$ P Waves

by

Hartmut Krasemann

Deutsches Elektronen-Synchrotron DESY, Hamburg

Abstract

We discuss angular distributions and some kinematic features for jets originating from the decay of orbitally excited $Q\bar{Q}$ states. These can be produced in e^+e^- storage rings via the radiative decay of the first radial excited $Q\bar{Q}$ vector meson.

We further present the complete and explicit angular distribution for the cascade decay $e^+e^- \to 2^3S_1 \to \gamma_1 + {}^3P_j$, ${}^3P_j \to \gamma_2 + 1^3S_1$, $1^3S_1 \to \mu^+\mu^-$ in all cases j=0,1,2. These distributions serve as a test of the spin j of intermediate states in $Q\bar{Q}$ systems. By the photon - gluon analogy they can successfully be applied to the jet process, too.

1. Introduction

The currently most promising candidate for a theory of the strong interactions is Quantum Chromo Dynamics, QCD, a nonabelian gauge theory of coloured quarks and eight coloured massless spin-1 gauge bosons, the gluons [1]. Asymptotic freedom [2] denotes the fact that the coupling constant α_s tends to zero for high momentum or short distance processes. Since resonance decays of the heavy hidden flavour states like J/ψ, Υ,..., which can be produced in electron positron annihilation in present (DORIS, SPEAR) or future (PETRA, PEP, CESR) machines, are short distance effects, they are hoped to be governed by a small α_s [3]. This allows to calculate strong decays in a way almost identical to electromagnetic decays of QED bound states, additionally only taking into account the nonabelian structure of QCD, especially the gluon self coupling [4]. However, long distance or small q^2 effects, like e.g. the hadron spectrum, need a better than the present understanding of the confinement regime, where the coupling constant α_s grows above 1 and forbids single quarks and gluons to separate and show up as free particles. For these effects one is forced to build phenomenological models like the bag [5] or potential models [6,7].

The confinement of the basic constituents has one important consequence. We cannot confirm the theory by observation of the quarks and gluons. We will probably never see a single quark or gluon. Any other evidence for the constituents from the spectrum of hadrons is rather indirect.

What would we know of QED if we had only hydrogen, positronium, myonium, etc. but no free electrons and photons?

But there is a surrogate for the observation of the free constituents, that are the jets. Experimentally jets are observed not only in deep inelastic hadron-hadron and lepton-hadron scattering but especially in e^+e^- annihilation, once the c.m. energy of 5 GeV is exceeded. The angular distribution of these jets is completely consistent with the production of two spin 1/2 (almost) massless particles [8], the quarks, via photon vacuum polarisation (see Fig. 1). The fragmentation of quarks into hadrons is imagined as a nonperturbative (and noncalculable → confinement) effect, which conserves the original directed momenta.

At present there is no way of calculating this process, but there exists a very suggestive picture: Inside a small space region of $\approx 1/2$ fm colour can exist and within this region the $q\bar{q}$ pair (or gluon) production is a short distance effect (see Fig. 2). When hard coloured quanta (quarks or gluons) with momenta $\vec{p}_i$ reach the confinement sphere they must fragment into white hadrons since colour fields cannot exist outside this sphere. The coloured quanta break up into hadrons with a finite perpendicular momentum $\vec{p}_\perp$. This breaking up is energetically much favoured over a further existence as coloured quanta. When the perpendicular momenta are small compared to the longitudinal hadron momenta, which add up to the momentum of the original quantum, we see hadron jets. The confinement effects, however, are assumed to be soft, carried by long wavelength quarks and/or gluons. The wavelength corresponds to the colour bag of 1/2 fm. Therefore the jet momenta equal the original quantum momenta up to the order of 400 MeV. This picture demands the production of the original jet quanta to be a short

distance effect ($\ll$ 1/2 fm). This is certainly true for the (electromagnetic) quark pair production in e^+e^-. It is also true for a hard gluon bremsstrahlung process [9]. Resonance decays, however, are not pointlike but involve propagators (Fig. 3). Here it is not so clear, how well the jet picture will work. However, because the propagators are mass dependent the picture will work the better the higher the mass of the decaying $Q\bar{Q}$ resonance is. For a Q-mass of 5 GeV the propagator length in Fig. 3 is probably already short enough to apply the jet picture and for the next new flavour (higher) $Q\bar{Q}$ resonance it will definitely be so (Fig. 4).

The quark jets in e^+e^- annihilation became visible above $s = (p_1+p_2)^2 \gtrsim (5\ \text{GeV})^2$, i.e. a massless quark needs $\gtrsim$2.5 GeV of energy against the c.m. to be able to form a jet. For gluons the jet threshold certainly is not lower. But a gluon carries the colour indices of a quark antiquark pair and each index may fragment separately. Then the multiplicity of the jet may be higher and the longitudinal hadron momenta may be lower. In the limit of asymptotic energies the gluon may just fragment like a $q\bar{q}$ pair, each quark carrying half the gluon momentum [10]. From this picture follows that a gluon jet of a certain longitudinal momentum will have a higher multiplicity and a larger opening angle than a quark jet of the same momentum. The threshold for gluon jet production will be higher than that for quark jet production with an upper bound of two times the quark threshold [+].

Up to now a lot of work was invested in the three gluon jet decay of heavy

[+] Speaking of a jet threshold we refer to the energy of a single quark or gluon versus the center of mass of the colour bag.

resonances in e^+e^- [10,11]. As far as the Y [12,13] decays are concerned, there is the problem that the average gluon energy in the 3 g decay of Y is only 3 GeV, which might be to low to observe the gluon jets, especially the 'star' configuration. Then the three gluon jets are left for the next $Q\bar{Q}$ resonance. [+)]

There is another source of gluon jets in $Q\bar{Q}$ decayswhich is much more likely to be accessible already in the Y system (and present in the $Q\bar{Q}(30)$ system, too). The ^3P_j waves of Y with spin j = 0, 1, 2 can be produced via $Y' \longrightarrow \gamma + {}^3P_j$ and they decay into two gluon ($^3P_{0,2}$) or quark ($^3P_1$) jets only. Observation of the quark jets of the $^3P_1$ decay should not be a problem and the gluon jets of the $^3P_{0,2}$ decays lie just at the upper bound of the jet threshold of our intuitive picture discussed above, they have a distinct energy of 5 GeV each. An experimental analysis of the gluon/quark jets can test theoretical predictions for the gluon angular distributions [14,15]. We will demonstrate in this paper, that in the decays of the $^3P_2$ and the $^3P_1$ states of heavy $Q\bar{Q}$ systems like the Y system or $Q\bar{Q}(30)$ there are clear tests of the gluon spin and masslessness (more precise: tests of the transverse gluon polarisations). In chapter 2 we write down the general matrix element for $^3P_j \longrightarrow 2$ gluons for arbitrary gluon masses. This is specialized to massless gluons and to the decay $^3P_{0,2} \longrightarrow 2g$ in chapter 3. By insertion of the quark vacuum polarisation for one gluon we specialize it to the process $^3P_1 \longrightarrow gg^* \longrightarrow g(q\bar{q})$ in chapter 4. As a by-product we obtain all the well known rates for $^1S_0 \longrightarrow gg$, $^3P_j \longrightarrow gg, gq\bar{q}$ [4)]. In the appendix we note the very useful explicit angular distribution formulae for the photon double cascade $e^+e^- \longrightarrow 2^3S_1 \longrightarrow \gamma_1 + {}^3P_j \longrightarrow \gamma_1 + \gamma_2 + {}^3S_1$ with intermediate spin j = 0, 1, 2. These angular distributions, written in helicity amplitudes, can easily be specified and applied to the decays of chapter 3 and 4. This leads to the angular distributions given there. It serves also to calculate angular distributions of alternative mechanisms. We close with a discussion of the

---

[+)] Since many theorists expect the next $Q\bar{Q}$ resonance at 20....30 GeV, let us nail down $Q\bar{Q}(30)$ as a working hypothesis.

results, an estimate of branching ratios for the interesting Y' decays and a quick outlook to the next $Q\bar{Q}$ resonance.

2. The Matrix Element of 2 Gluon Decay

In the nonrelativistic approximation to the decay of a bound $Q\bar{Q}$ pair into two gluons the decay amplitude (Fig. 5b)

$$\mathcal{M} = -\sqrt{\tfrac{2}{3}}\, 4\pi\alpha_s \int d^4q\ Tr\left[\Psi(P,q)\, N(P,q)\right] \tag{2.1}$$

factorizes into the amplitude of annihilation of a free $Q\bar{Q}$ pair of quark mass m_Q and momenta $P/2 + q$ and $P/2 - q$ into two gluons of momenta k_1 and k_2

$$N(P,q) = \not{\varepsilon}_2 \frac{\not{P}/2 + \not{q} - \not{k}_1 + m_Q}{k_1\cdot k_2 - q\cdot(k_2 - k_1)} \not{\varepsilon}_1 + \not{\varepsilon}_1 \frac{\not{P}/2 + \not{q} - \not{k}_2 + m_Q}{k_1\cdot k_2 - q\cdot(k_1 - k_2)} \not{\varepsilon}_2 \tag{2.2}$$

and the Bethe Salpeter amplitude to find Q and $\bar{Q}$ with the required momenta in the bound state, here in covariant notation:

$$\Psi(P,q) = \frac{-1}{4 m_Q^2} \left(\not{P}/2 + \not{q} + m_Q\right) \not{\varepsilon} \left(\not{P}/2 - \not{q} - m_Q\right) . \tag{2.3}$$

P is the bound state momentum, q the relative $Q\bar{Q}$ momentum and ε the non-relativistic polarisation tensor:

$$S,\ j^{PC}=0^{++} \qquad \not\epsilon_S = \frac{1}{\sqrt{2}}\left(\hat{\not q} - \hat{q}\cdot\hat{P}_S \not P_S\right)\frac{R_S(\vec q)}{\sqrt{4\pi}}\,\delta(q_0) \tag{2.4}$$

$$A,\ j^{PC}=1^{++} \qquad \not\epsilon_A = \sqrt{\frac{3}{4}}\,\epsilon(\epsilon_{S_z}, \hat q, \hat P_A, \gamma)\frac{R_A(\vec q)}{\sqrt{4\pi}}\,\delta(q_0) \tag{2.5}$$

$$T,\ j^{PC}=2^{++} \qquad \not\epsilon_T = \sqrt{\frac{3}{2}}\,\epsilon^{\mu\nu}\hat q_\mu \gamma_\nu \frac{R_T(\vec q)}{\sqrt{4\pi}}\,\delta(q_0) \tag{2.6}$$

$$PS,\ j^{PC}=0^{-+} \qquad \not\epsilon_{PS} = \frac{1}{\sqrt{2}}\,\gamma_5 \hat{\not P}_{PS}\frac{R_{PS}(\vec q)}{\sqrt{4\pi}}\,\delta(q_0) \tag{2.7}$$

with the radial Schrödinger wave functions $\int |\vec q|^2 d|\vec q|\,|R(\vec q)|^2 = 1$.
The couplings in decays involving gluons are not just multiplicative but more complicated because of the nonabelian character of QCD . The gluons carry colour charge $1/2\ g_s \lambda^a_{ij}$, g_s being the strong coupling, $g_s^2 = 4\pi\alpha_s$
The λ^a_{ij} are the eight 3 x 3 Gell-Mann λ matrices, a = 1, ... 8, with the colour indices i, j = 1, 2, 3. Each λ^a corresponds to one gluon which thus carries the colour of a quark-antiquark pair i and j. The two gluons of Fig. 5 have to be in a colour singlet state, therefore one has to contract the colour indices of gluon 1 and 2, $\lambda^a_{ij}\cdot\lambda^b_{ij} = Tr\left[\lambda^a\cdot\lambda^b\right]$. In the squared matrix element we have to sum over all indices a and b, obtaining [16]

$$\sum_{a,b}\ \frac{1}{\sqrt{3}}\,Tr\left(\frac{\lambda^a}{2}\cdot\frac{\lambda^b}{2}\right)\ \frac{1}{\sqrt{3}}\,Tr\left(\frac{\lambda^{*a}}{2}\cdot\frac{\lambda^{*b}}{2}\right) \;=\; \frac{2}{3} \tag{2.8}$$

Since $Tr[\lambda^a \lambda^b] = 2\,\delta^{ab}$. The factor $1/\sqrt{3}$ stems from the normalisation of the $Q\bar{Q}$ colour wave function. We now consider an expansion of N(2.2) and Ψ(2.3) in powers of q. (2.1) indicates the loop integration over q which will be reduced to an integral over the Schrödinger wave function in momentum space because of $\delta(q_0)$. In the 0th order in q we will be left with $\int d^3\vec{q}\, R(\vec{q}) = R(\vec{r} = 0)$, this lowest order can only contribute to S wave decays. P waves have a vanishing Schrödinger wave function at the origin and therefore we have to expand $N \cdot \Psi(q)$ to the first order in q, which leads us to loop integrals of the form $\left(\hat{q}\, R(\vec{q})/\sqrt{4\pi} \equiv \vec{\varphi}(\vec{q}) \right)$

$\int d^3q\, q^i \hat{q}^j R(\vec{q}) = \sqrt{4\pi} \int d^3q\, q^i \varphi^j(\vec{q}) = \sqrt{4\pi}\, \delta^{ij}\, \varphi'(\vec{r}=0) =$

$= \delta^{ij}\, R'(\vec{r}=0)$ with the nonvanishing derivative of the spatial Schrödinger wave function at the origin.

The expansion of $N \cdot \Psi(q)$ leads in 0th order to

$$\left[\Psi(q) \cdot N(q)\right]^{(0)} = \frac{m_Q^2}{(k_1 \cdot k_2)^2} \left(\varepsilon_1 \cdot \varepsilon_2\, \not\varepsilon \not P - \frac{1}{2} \not\varepsilon \left(\not\varepsilon_2 \not k \not\varepsilon_1 - \not\varepsilon_1 \not k \not\varepsilon_2 \right) \right) \tag{2.9}$$

and in first order to

$$\begin{aligned} \left[\Psi(q) \cdot N(q)\right]^{(1)} = \frac{1}{(k_1 \cdot k_2)^2} \Bigg[& \frac{1}{4}\, q \cdot k\, \not\varepsilon \not P \left(\not\varepsilon_2 \not\varepsilon_1 - \not\varepsilon_1 \not\varepsilon_2 \right) \\ & - \frac{1}{2}\, q \cdot k\, \not\varepsilon \left(\not\varepsilon_2\, \varepsilon_1 \cdot k + \not\varepsilon_1\, \varepsilon_2 \cdot k - \not k\, \varepsilon_1 \cdot \varepsilon_2 \right) \\ & - 2\, m_Q^2 \left(\not\varepsilon \not\varepsilon_1 \varepsilon_2 \cdot q + \not\varepsilon \not\varepsilon_2 \varepsilon_1 \cdot q - \not\varepsilon \not q\, \varepsilon_1 \cdot \varepsilon_2 + q \cdot \varepsilon\, \varepsilon_1 \cdot \varepsilon_2 \right) \\ & + \frac{1}{4}\, q \cdot \varepsilon\, \not P \left(\not\varepsilon_2 \not k \not\varepsilon_1 - \not\varepsilon_1 \not k \not\varepsilon_2 \right) \\ & + \frac{1}{4}\, \not P \not q \left(\not\varepsilon_2 \not k \not\varepsilon_1 - \not\varepsilon_1 \not k \not\varepsilon_2 \right) \not\varepsilon \Bigg] \end{aligned} \tag{2.10}$$

Here $k \equiv k_2 - k_1$ and the state polarisation vector $\not{\varepsilon}$ is allowed to be of the $\gamma_5 \gamma_\mu$ type (e.g. pseudoscalars) or the γ_μ type (e.g. vectors). For $\not{\varepsilon}$ of γ_μ type, the trace of (2.9) vanishes, especially the vector ground state does not decay into two gluons. But the pseudoscalar ground state does and with $\not{\varepsilon}_{PS}$ from (2.7) one finds for massless gluons ($k_1^2 = 0$, $k_1 \cdot k_2 = 2\, m_Q^2$)

$$Tr\left[\psi \cdot N(q)\right]^{(0)}_{PS} = \frac{1}{m_Q^2}\, \epsilon(\hat{P}_{PS}, \varepsilon_2, k, \varepsilon_1)\, \frac{1}{\sqrt{2}}\, \frac{R_{PS}(\vec{q})}{\sqrt{4\pi}}\, \delta(q_0) \qquad (2.11)$$

Inserting this in (2.1) and performing the square and the polarisation sum gives

$$\sum_\lambda |\mathcal{M}|^2 = \frac{2}{3}(4\pi\alpha_s)^2\, \frac{1}{2}\, \frac{|R_{PS}(0)|^2}{4\pi}\, \frac{8\, m_Q^2}{m_Q^4} \quad . \qquad (2.12)$$

With the width formula

$$\Gamma = \frac{P_{cm}}{4M}\, \frac{1}{2j_i + 1} \int \frac{d\Omega}{4\pi^2} \sum_\lambda |\mathcal{M}|^2 \cdot S \qquad (2.13)$$

the phase space $P_{cm} = M/2$, and the statistical factor $S = 1/2$! The pseudoscalar width is [17,4)]

$$\Gamma(PS \to 2g) = \frac{2}{3}\alpha_s^2 \frac{|R_{PS}(0)|^2}{m_Q^2} \quad . \tag{2.14}$$

We now turn to states with $\not{\varepsilon}$ of the γ_μ type. These are the P waves (2.4)...(2.6). For these (2.9) vanishes and the trace of (2.10) gives

$$\begin{aligned} Tr\left[\Psi \cdot N(q)\right]^{(1)} = \frac{2}{(k_1\cdot k_2)^2}\Big[& -2k_1\cdot k_2\,(\varepsilon\cdot\varepsilon_1\, q\cdot\varepsilon_2 + \varepsilon\cdot\varepsilon_2\, q\cdot\varepsilon_1) \\ & + q\cdot k\,(2\,\varepsilon\cdot\varepsilon_1\, k_1\cdot\varepsilon_2 - 2\,\varepsilon\cdot\varepsilon_2\, k_2\cdot\varepsilon_1 + \varepsilon_1\cdot\varepsilon_2\,\varepsilon\cdot k)\Big] \\ + \frac{1}{m_Q^2\,(k_1\cdot k_2)}\Big[& k\cdot q\,(P\cdot\varepsilon_1\,\varepsilon\cdot\varepsilon_2 - P\cdot\varepsilon_2\,\varepsilon\cdot\varepsilon_1) \\ & + \varepsilon\cdot k\,(P\cdot\varepsilon_2\, q\cdot\varepsilon_1 - P\cdot\varepsilon_1\, q\cdot\varepsilon_2) \\ & + P\cdot k\,(\varepsilon\cdot\varepsilon_1\, q\cdot\varepsilon_2 - \varepsilon\cdot\varepsilon_2\, q\cdot\varepsilon_1)\Big] \\ + \frac{\varepsilon\cdot P}{m_Q^2\,(k_1\cdot k_2)^2}\Big[& k_1\cdot k_2\,(P\cdot\varepsilon_2\, q\cdot\varepsilon_1 + P\cdot\varepsilon_1\, q\cdot\varepsilon_2 - P\cdot q\,\varepsilon_1\cdot\varepsilon_2 \\ & + \tfrac{1}{2}\,k\cdot q\,(P\cdot\varepsilon_2\, k\cdot\varepsilon_1 + P\cdot\varepsilon_1\, k\cdot\varepsilon_2 - P\cdot k\,\varepsilon_1\cdot\varepsilon_2)\Big] \quad . \end{aligned} \tag{2.15}$$

In this expression $P\cdot q = 0$ for the quarks on mass shell, while the Lorentz condition gives $\varepsilon\cdot P = 0$. For massless gluons we furthermore have $k\cdot P = 0$.

3. The Decays $^3P_{0,2} \longrightarrow gg$

The $Q\bar{Q}$ P waves with spin 0 and 2 can both decay into a pair of gluons according to Fig. 5. Inserting their polarisation tensor (2.4) or (2.6) resp. in (2.15), only the symmetric terms survive:

$$Tr\left[\not{\varepsilon}\, N(q)\right]^{(1)}_{j=0,2} = \frac{2}{(k_1\cdot k_2)^2}\Big[-4\,k_1\cdot k_2\;\varepsilon\cdot\varepsilon_1\; q\cdot\varepsilon_2 + q\cdot k\,(\varepsilon\cdot k\;\varepsilon_1\cdot\varepsilon_2 - 2\,\varepsilon\cdot\varepsilon_1\;k\cdot\varepsilon_2 - 2\,\varepsilon\cdot\varepsilon_2\;k\cdot\varepsilon_1)\Big]. \tag{3.1}$$

Until now the gluons were allowed to carry arbitrary masses. We now specify to the approximation of massless gluons ($k_1 \cdot k_2 = 2m_Q^2$) and compute from (3.1) for the decay of the Scalar (using (2.4)):

$$\sum_\lambda |\mathcal{M}_{0^{++}}|^2 = \frac{2}{3}(4\pi\alpha_s)^2\,\frac{1}{2}\cdot\frac{|R'_S(0)|^2}{4\pi}\,\frac{72}{m_Q^4}\quad, \tag{3.2}$$

which leads to the well known result [4]

$$\Gamma(0^{++}\longrightarrow 2g) = 6\,\alpha_s\,\frac{|R'_S(0)|^2}{m_Q^4}\quad. \tag{3.3}$$

The decay of the Tensor (using (2.6)) is [4]

$$\sum_\lambda |\mathcal{M}_{2^{++}}|^2 = \frac{2}{3}(4\pi\alpha_s)^2\,\frac{3}{2}\,\frac{|R'_T(0)|^2}{4\pi}\,\frac{32}{m_Q^4}\quad, \tag{3.4}$$

$$\Gamma(2^{++} \longrightarrow 2g) = \frac{8}{5}\,\alpha_s^2\,\frac{|R_T'(0)|^2}{m_Q{}^4} \quad . \tag{3.5}$$

Yet in case of the tensor the matrix element (3.1) contains more information than only this. After doing the q-loop integration, but before squaring the matrix element and summing over polarisations, one finds [14]

$$\mathcal{M}_{2^{++}} \sim \varepsilon_{j_3}^{\mu\nu}\left(k_1\cdot k_2\;\varepsilon_{1\mu}^{*}\,\varepsilon_{2\nu}^{*} + \varepsilon_1^{*}\cdot\varepsilon_2^{*}\,k_{1\mu}\,k_{2\nu}\right) . \tag{3.6}$$

Inserting the 2^{++}-polarisation tensor which in the c.m.s. reads

$$\varepsilon_0 = \frac{1}{\sqrt{6}}\begin{vmatrix} 0 & 0 & 0 & 0 \\ 0 & -1 & 0 & 0 \\ 0 & 0 & -1 & 0 \\ 0 & 0 & 0 & 2 \end{vmatrix}, \quad \varepsilon_{\pm 1} = \frac{1}{2}\begin{vmatrix} 0 & 0 & 0 & 0 \\ 0 & 0 & 0 & \mp 1 \\ 0 & 0 & 0 & -i \\ 0 & \mp 1 & -i & 0 \end{vmatrix}, \quad \varepsilon_{\pm 2} = \frac{1}{2}\begin{vmatrix} 0 & 0 & 0 & 0 \\ 0 & 1 & \pm i & 0 \\ 0 & \pm i & -1 & 0 \\ 0 & 0 & 0 & 0 \end{vmatrix}, \tag{3.7}$$

(3.6) vanishes for $j_3 = \pm 1$ and $j_3 = 0$. It only survives for $j_3 = \pm 2$. Note that this conjecture only holds for massless gluons. It is clear that two massless collinear gluons cannot form a helicity ± 1 state, but it is nontrivial that the helicity 0 state of the $^3P_2$ resonance does not contribute to the decay. The experimental verification that the helicities ± 2 dominate in the decay would test that gluons really behave as massless (transversely polarized) spin 1 particles on short distances. Our nonrelativistic approximation to the 2^{++} wave fuction and the $\gamma_\mu$gluon - quark coupling are of course also tested. The test is carried out by measuring the angular distributions in (Fig. 6)

$$e^+e^- \longrightarrow V' \longrightarrow \gamma + {}^3P_2 \longrightarrow \gamma + 2g \longrightarrow \gamma + 2\,\text{jets} \tag{3.8}$$

in the angles according to Fig. 9. The kinematics of the helicity ± 2 states give (compare the Appendix)

$$W_{2^{++}}^{\lambda=\pm 2}(\theta, \varphi, \theta_{\gamma j}) \sim (1+\cos^2\theta_{\gamma j})^2 (1+\cos^2\theta) + 2(1-\cos^4\theta_{\gamma j}) \sin^2\theta + (1+\cos^2\theta_{\gamma j})(\sin 2\theta_{\gamma j} \sin 2\theta \cos\varphi + \sin^2\theta_{\gamma j} \sin^2\theta \cos 2\varphi), \tag{3.9}$$

and integrated over θ, φ,

$$W_{2^{++}}^{\lambda=\pm 2}(\theta_{\gamma j}) \sim 1+\cos^2\theta_{\gamma j} \tag{3.10}$$

To contrast this distribution to alternative cases like a direct coupling of the 2^{++} to a $q\bar{q}$ pair or to scalar particles, we note the angular distributions of the helicity 0 and ± 1 decays with the weight A for helicity ± 1 over helicity 0 (again compare the Appendix) [14]

$$\begin{aligned} W_{2^{++}}^{\lambda=0,\pm 1}(\theta, \varphi, \theta_{\gamma j}) \sim & \left[A^2(2+2\cos^2\theta_{\gamma j} - 4\cos^4\theta_{\gamma j}) + \left(\tfrac{10}{3} - 8\cos^2\theta_{\gamma j} + 6\cos^4\theta_{\gamma j}\right)\right](1+\cos^2\theta) \\ & + \left[A^2(2-6\cos^2\theta_{\gamma j} + 8\cos^4\theta_{\gamma j}) + 12(\cos^2\theta_{\gamma j} - \cos^4\theta_{\gamma j})\right] \sin^2\theta \\ & + \left[A^2(1-4\cos^2\theta_{\gamma j}) - (4-6\cos^2\theta_{\gamma j})\right] \sin 2\theta_{\gamma j} \sin 2\theta \cos\varphi \\ & - \left[A^2 4\cos^2\theta_{\gamma j} + (2-6\cos^2\theta_{\gamma j})\right] \sin^2\theta_{\gamma j} \sin^2\theta \cos 2\varphi. \end{aligned} \tag{3.11}$$

and again integrated over θ, φ

$$W_{2^{++}}^{\lambda=0,\pm1}(\theta_{\gamma j}) \sim 1 - \alpha \cos^2\theta_{\gamma j} \,, \qquad \alpha = \frac{6+3A^2}{10+9A^2} \,. \tag{3.12}$$

The sign in (3.12) is always negative with $1/3 \leq \alpha \leq 3/5$ in contrast to (3.10). This allows to clearly distinguish the helicities ± 2 from helicities $0, \pm 1$ in the decay amplitude and we have thus found one clear test for QCD.

4. The Decay $^3P_1 \longrightarrow gq\bar{q}$

We will discuss the $^3P_1$ decay assuming massless gluons from the beginning. A spin 1 particle like the $^3P_1$, however, cannot decay into two massless gluons. The next order processes are shown in Fig. 7. There is one diagram (Fig. 7c) for $^3P_1 \longrightarrow gq\bar{q}$ and two diagrams (Fig. 7a, b) for $^3P_1 \longrightarrow 3g$. Barbieri, Gatto and Remiddi [4] found that the diagrams Fig. 7a and Fig. 7b almost cancel and that their remaining contribution is negligible. Okun and Voloshin [4] gave the general argument for this cancellation: Consider the annihilation of a free $Q\bar{Q}$ pair. One of the massless gluons, say g_1, is a Bremsstrahlungs gluon when it carries away the angular momentum of the initial $Q\bar{Q}$ pair. The amplitudes Fig. 7a, b, c therefore show the typical Bremsstrahlung singularity. Now we take into account that amplitudes Fig. 7a and Fig. 7b interfere, since they lead to the same final state. Further we know from QED that the singular part of (a+b) factorizes in the Bremsstrahlung part times the remaining non-singular decay amplitude of a coloured ($^3S_1$) $Q\bar{Q}$ state into two massless gluons. Since the latter amplitude is zero, the singularities of (a+b) must

cancel. The dominant contribution to the $^3P_1$ decay will therefore arise from the singular part of diagram Fig. 7c. Of course this singularity is cut off by the bound state wave function of the $^3P_1$ state. The existence of such a cutoff already follows from the fact that colour is confined to a space region of $\approx 1/2$ fm in diameter. This length coincides with the extension of the P waves in the Υ system as well as in the charmonium system. It therefore seems to be reasonable to cut the singularity of diagram Fig. 7c at a minimal energy of $K_{min} \approx 400$ MeV for the soft Bremsstrahlung gluon. For heavier $Q\bar{Q}$ resonances beyond Υ the size of the system becomes smaller than the confinement size. Then K_{min} increases over 400 MeV and can be estimated as in corresponding QED decays [4].
The described cutoff procedure, however, is not gauge invariant but we hope that gauge invariance is restored by higher order graphs like vertex corrections etc. as in QED [4].

The decay $^3P_1 \longrightarrow gq\bar{q}$ is a three body decay[+] and therefore significantly different from competing processes like a direct coupling to a $q\bar{q}$ pair, which would be a two body decay. We will qualify later that this feature gives a unique characteristic to the structure of the events. In a small subsample of all events there will be two non collinear quark jets recoiling against a gluon [++]. Most of all events, however, will have two almost collinear quark jets and one soft gluon which should not fragment in a jet.

[+] Note that these $q\bar{q}$ jets are $c\bar{c}$ a quarter of the time since the quark couples by its colour, not its electric charge.

[++] In Υ' decays this gluon will be too soft to form a jet itself but in corresponding $Q\bar{Q}$ (30 GeV) decays it will give rise to a three jet configuration in a fraction of all events.

To calculate the width and the helicity amplitudes of $^3P_1 \longrightarrow gq\bar{q}$ we now use the general matrix element of chapter 2. From (2.15) follows the width Γ_a of $^3P_1$ into one massless and one massive ($m = \sqrt{a}$) gluon. The matrix element reads after insertion of (2.5) and q-integration

$$\mathcal{M}^{a}_{1^{++}} = i\sqrt{\frac{2}{3}}\,4\pi\alpha_s\,\frac{\sqrt{3}}{2}\,\frac{R'_A(0)}{\sqrt{4\pi}}\,\frac{2}{(k_1\cdot k_2)^2}\,\frac{1}{m_Q^2}\,\times$$
$$\times\Big[\,\varepsilon_2\cdot(2m_Q^2 k_1 - k_1\cdot k_2\,P_A)\;\in(\varepsilon_1,\varepsilon_{S_3},k,\hat{P}_A)$$
$$-\,\varepsilon_1\cdot(2m_Q^2 k_2 - k_1\cdot k_2\,P_A)\;\in(\varepsilon_2,\varepsilon_{S_3},k,\hat{P}_A) \qquad (4.1)$$
$$+\,k_1\cdot k_2\;P_A\cdot k\;\in(\varepsilon_1,\varepsilon_{S_3},\varepsilon_2,\hat{P}_A)\Big]$$

Squaring and summing over the polarisations gives, when $k_1^2 = 0$ and $k_2^2 = a$ [18],

$$\sum_\lambda |\mathcal{M}^{a}_{1^{++}}|^2 = \frac{2}{3}(4\pi\alpha_s)^2\frac{3}{4}\,\frac{|R'_A(0)|^2}{4\pi}\,\frac{32a(M^2+a)}{m_Q^4\,(M^2-a)^2} \qquad (4.2)$$

The width follows from (2.13) (here S = 1)

$$\Gamma_a\;(1^{++}\longrightarrow g\,g^*) = \frac{2}{3}\,\alpha_s^2\,\frac{4a(M^2+a)}{M^2 m_Q^4(M^2-a)}\,|R'_A(0)|^2 \qquad (4.3)$$

The term $\sim a$ in the numerator of (4.2) and (4.3) comes from the transverse helicities of the massive gluon, the term $\sim M^2$ comes from 0 helicity. In the limit of high gluon masses $\sqrt{a} \simeq M$ both terms contribute equally. This

corresponds to an electric dipole pattern. For small a the 0 helicity of the massive gluon dominates (because the transverse helicities are strictly forbidden in the limit $a \to 0$).

Inserting the imaginary part of the gluon $q\bar{q}$ vacuum polarisation

$$Im\ \tilde{\Pi}^{(2)}_{q\bar{q}}(a) = \sum_1^n{}_q \frac{\alpha_s}{6}\left(1+\frac{2m_q^2}{a}\right)\sqrt{1-\frac{4m_q^2}{a}}\ \theta(a-4m_q^2), \qquad (4.4)$$

written as a sum over the light quark flavour q, and integrating over a gives (compare Fig. 10)

$$\Gamma(1^{++} \longrightarrow g\,q\bar{q}) = \frac{1}{\pi}\int da\ \Gamma_a(1^{++} \longrightarrow gg^*)\ Im\ \tilde{\Pi}^{(2)}_{q\bar{q}}(a)\,. \qquad (4.5)$$

For each quark flavour the vacuum polarisation (4.4) is down by a factor 1/2 compared to the abelian case (QED). This simply is the algebra $\sum_b g\lambda^a_{ij}/2 \cdot g\lambda^b_{ij}/2 = \sum_b \tfrac{1}{4} g^2\, Tr(\lambda^a\lambda^b) = \tfrac{1}{2} g^2$. We now expand (4.4), neglect terms $\sim m_q^2/a$, m_q^2/M^2 and find (compare Fig. 11 for the integrand):

$$\Gamma(1^{++} \longrightarrow q\bar{q}q\bar{q}) = \sum_1^n{}_q \frac{8\alpha_s^3\,|R_A'(0)|^2}{9\pi\ m_Q^4}\int_{4m_q^2}^{M^2-\Delta} da\ \frac{M^2+a}{2M^2(M^2-a)}$$

$$\simeq \frac{n}{3}\ \frac{8\alpha_s^3\,|R_A'(0)|^2}{3\pi\ m_Q^4}\left(\ln\frac{M^2}{\Delta} - \frac{1}{2}\left(1-\frac{\Delta}{M^2}\right)\right). \qquad (4.6)$$

We have cut off the integration at $M^2 - \Delta$ which corresponds to a lower limit on the energy of the soft gluon of $k_{min} = \frac{1}{2} \frac{\Delta}{M}$.

The angular distribution for the process (Fig. 8)

$$e^+e^- \longrightarrow V' \longrightarrow \gamma + {}^3P_1 \longrightarrow \gamma + g\,q\bar{q} \longrightarrow \gamma + g + 2jets \qquad (4.7)$$

depends on the ratio A of helicity ± 1 / helicity 0 of the massive gluon which in turn depends on its mass $\sqrt{\alpha}$. In Fig. 11 the differential rate $d\Gamma/d\alpha$ and the contributions of the two helicity amplitudes are shown. As a function of A we find [18] (compare the Appendix)

$$W^{gq\bar{q}}_{1++}(\theta_{e\gamma}, \theta_{ej}, \theta_{\gamma j}) \sim 5(A^2+1) - (2A^2+A+2)\cos^2\theta_{e\gamma} + (A^2+3A+1)\cos\theta_{e\gamma}\cos\theta_{\gamma j}\cos\theta_{ej} \qquad (4.8)$$

with the angles $\theta_{e\gamma}$ between beam and photon, θ_{ej} between beam and jet, $\theta_{\gamma j}$ between photon and jet. (4.8) is symmetric against reversion of the beam axis or the jet axis, but for the definition of these angles one has to take the same side of the beam (say e^-) and the same arm of the jets. Another warning corresponds to the frames in which the angles are measured: $\theta_{e\gamma}$ is in the lab frame, but θ_{ej} and $\theta_{\gamma j}$ are measured in the c.m.s. of the two quark jets!

In the kinematical range $\alpha \gtrsim (M/2)^2$ we have $1 < A \lesssim 2$ and the angular distribution varies very slowly. In this range

$$W^{g q\bar{q}}_{1^{++}}(\theta_{eg}, \theta_{ej}, \theta_{gj}) \simeq 2 - \cos^2\theta_{eg} + \cos\theta_{eg}\cos\theta_{ej}\cos\theta_{gj} \quad (4.9)$$

up to 10 %. For the $^3P_1$ decay in the Υ system any event in which the quarks form jets fall within this range.

To compare this distribution to an arbitrary two-body decay (e.g. $q\bar{q}$) we note the angular distribution of the latter again as a function of

A = helicity $\pm$ 1 / helicity 0

$$W^{q\bar{q}}_{1^{++}}(\theta_{eg}, \theta_{ej}, \theta_{gj}) \sim (1+A^2) - \cos^2\theta_{eg} + (2-A^2)\cos\theta_{eg}\cos\theta_{ej}\cos\theta_{gj} \quad (4.10)$$

In the case of a decay of the 1^{++} in two spinless particles A = 0 and in case of a decay into <u>massless</u> quarks $A = \infty$ [15].

The main difference between the process (4.7) and alternative processes is, however, that in (4.7) the quark jets stem from the heavy gluon which carries a considerable acount of energy. Therefore the two quark jets of process (4.7) recoil against the momentum p_{boost} of the soft gluon and will in general not be collinear, whereas in two body decays of the 1^{++} as well as in the decays of the 0^{++} and 2^{++} the recoil momentum of the trigger photon will only slightly change the collinearity of the two jets, by at most 10 degrees. To simplify the discussion we pick out events with $0.5 \lesssim a/M^2 \lesssim 0.8$ (compare Fig. 11). In the Υ system this corresponds to 7 GeV $\lesssim \sqrt{\alpha} \lesssim$ 9 GeV and

$0.95\ \text{GeV} \leq p_{boost} \leq 2.55\ \text{GeV}$. This range contains $\approx 35\ \%$ of all events. From this sample we pick those events where the quark momenta are almost perpendicular to the boost in the rest frame of the heavy gluon. For these events the opening angle in the lab frame is easily calculated and we find $\theta_{q\bar{q}}$ in the range $110^0 \leq \theta_{q\bar{q}} \leq 160^0$, much smaller than $170^0 < \theta_{q\bar{q}} \leq 180^0$ for any imaginable other process. In the Υ system the energy of the recoiling (soft) gluon is not sufficient for the formation of a third jet, it will just lead to a central cluster of recoiling soft hadrons (Fig. 8). In higher $Q\bar{Q}$ systems, however, the recoiling gluon sometimes leads to a third jet. This jet configuration is unique for the process (4.7), its experimental verification for a small subset of $^3P_1$ decays would test much more assumptions and features of QCD than the angular distributions alone.

5. Outlook on the Υ system and higher $Q\bar{Q}$ resonances.

From (3.3), (3.5) and (4.3) we find [4)]

$$\Gamma(0^{++}) : \Gamma(1^{++}) : \Gamma(2^{++}) = 15 : \frac{20\, n\, \alpha_s}{9\pi}\left(\ln\frac{M^2}{\Delta} - \frac{1}{2}\right) : 4 \qquad (5.1)$$

For α_s we take 0.4 at 3 GeV leading to $\alpha_s = 0.25$ at 10 GeV and $\alpha_s \simeq 0.2$ at 30 GeV. The number of quark flavours $n = 3$ for $c\bar{c}$ decays, 4 in Υ decays and would be 5 at $Q\bar{Q}(30)$. With the same $k_{min} \simeq 1/2\,\Delta/M \simeq 400$ MeV in all three cases for simplicity (5.1) becomes

$$\begin{aligned} &15 : 0.9 : 4 \quad \text{in the } J/\Psi \text{ system} \\ &15 : 1.4 : 4 \quad \text{in the } \Upsilon \text{ system} \\ &15 : 2.2 : 4 \quad \text{in the } Q\bar{Q}(30) \text{ system.} \end{aligned} \qquad (5.2)$$

In a detailed numerical analysis we find $|R'_{c\bar{c}}(0)|^2/m_c^4 \simeq 15$ MeV in charmonium and $|R'_{b\bar{b}}(0)|^2/m_b^4 \simeq 2.5$ MeV in the Υ system. Both quoted quantities are to a large extent quark mass independent. From (3.3), (3.5) and (4.3) we now calculate the widths of Table 1. Estimates for interesting branching fractions in the Υ system are given in Table 2. The results of Table 2 are based on the following scaling [19] estimates with J/ψ data as input.

The $\Upsilon' - \Upsilon$ splitting is as large as the $\psi' - J/\psi$ splitting [12]. We therefore also expect the c.o.g. of the P waves of the Υ system to lie ca. 160 MeV below Υ'. The P wave splitting, following the Fermi Breit Hamiltonian with the Coulomb part $V_c(r) = \frac{4}{3}\alpha_s/r$ of the potential alone, behaves as $m_Q^{-2}\langle \frac{1}{r}\partial_r V_c(r)\rangle$. The linear part of the potential, however, determines the length scale of the wave functions, $r \sim m_Q^{-1/3}$ and thus we find a m_Q^{-1} behaviour of the P wave splittings.

Υ:

$$M(^3P_2) - M(^3P_1) \simeq 20 \text{ MeV}$$
$$M(^3P_1) - M(^3P_0) \simeq 30 \text{ MeV} \qquad (5.3)$$

The radiative decay widths of Υ' into the P waves behave as $e_Q^2 k^3 k_{c.o.g}^{-1} m_Q^{-1}$, following the dipole sum rules. Since $k_{c.o.g} = 160$ MeV in both charmonium and the Υ system, we are left with $Q^2 k^3 m_Q^{-1}$. The leptonic decay of Υ' follows the Van Royen Weisskopf formula [20]

$$\Gamma_{e^+e^-}(V') = 4\alpha^2 e_Q^2 |R(0)|^2 M_{V'}^{-2} \qquad (5.4)$$

and scales like $e_Q^2 r^{-3} m_Q^{-2}$. $\Gamma_{e^+e^-}$ therefore scales like $e_Q^2 m_Q^{-1}$ in a pure linear potential and like $e_Q^2 m_Q$ in a pure coulombic potential. The wave function at the origin in (5.4) must feel more of the coulombic part of the potential than the dipole matrix element. Detailed numerical calculations show almost m_Q-independence, which is also supported by experiment, $e_c^2 \Gamma_{e^+e^-}(J/\psi) \simeq e_b^2 \Gamma_{e^+e^-}(\Upsilon)$. The total width via 1 γ annihilation is $(R + 2) \Gamma_{e^+e^-}$. The direct hadronic decay of Υ', Γ_{3g}, is related to $\Gamma_{e^+e^-}$ by $\Gamma_{3g} \sim \Gamma_{e^+e^-} \cdot \alpha_s^3 \cdot e_Q^{-2}$ and the $\pi\pi$ cascade decay into the ground state scales like m_Q^{-2} for constant phase space [21].

Putting everything together we find process (3.8) in ≈ 5 %, process (4.7) in ≈ 3 %, and the process analog to (3.8) involving the 0^{++} in ≈ 2 % of all Υ' decays. The branching fractions for corresponding decays of a 30 GeV $Q\bar{Q}$ resonance will not be much larger, even if this resonance should have $e_Q = 2/3$. This is because the hadronic decays become relatively unimportant. The unknown quantity which determines the branching fractions is the ratio of the wavefunction at the origin to the dipole matrix element.

The experimental problems in a P wave jet search (besides the small branching fractions) are i) the background process $\Upsilon' \rightarrow 2\pi^0 \Upsilon \rightarrow 1\gamma + X$ with only one γ from a π^0 decay detected and ii) the necessary photon resolution of $\ll 20$ MeV (compare (5.3)). While problem i) becomes unimportant at the $Q\bar{Q}(30)$ resonance (the cascade $2^3S_1 \rightarrow \pi\pi\ 1^3S_1$ there is negligible), problem ii) becomes more severe. The spin orbit splitting will decrease by another factor of three and be typical around 5 ... 10 MeV. Differentiating process (3.8) from (4.7) becomes even harder than in the Υ system.

6. Appendix

In this appendix we give the explicit angular distributions [22,23] for

$$e^+e^- \longrightarrow V_1 \longrightarrow \gamma_1 + \chi_j \longrightarrow \gamma_1 + \gamma_2 + V_2 \longrightarrow \gamma_1 + \gamma_2 + \mu^+\mu^- \qquad (6.1)$$

with j=0,1,2, following from the general formula of Karl,Meshkov and Rosner [22]. We will only describe this formula shortly and refer to Ref.(22) for a detailed discussion. The first part of the cascade, $e^+e^- \rightarrow V_1$, is determined by the γ_μ coupling of the s channel photon to the electron, neglecting the electron mass. The same is true for $V_2 \longrightarrow \mu^+\mu^-$. We now look at the intermediate states χ_j (e.g. ^3P_j in $c\bar{c}$ or $b\bar{b}$) with j = 0, 1, 2. The transitions to and from χ_j can be described by the helicity amplitudes

$$V_1(\lambda_1) \longrightarrow \gamma_1(\mu_1) + \chi_j(\nu_1)$$
$$B_{\nu_1,\mu_1}: \quad \lambda_1 = \mu_1 - \nu_1 \qquad (6.2)$$

and

$$\chi_j(\nu_2) \longrightarrow \gamma_2(\mu_2) + V_2(\lambda_2)$$
$$A_{\nu_2,\mu_2}: \quad \nu_2 = \mu_2 - \lambda_2 \qquad (6.3)$$

The helicity amplitudes A, B for $\mu_{1,2} = +1$ are related to those for $\mu_{1,2} = -1$ by parity, so that j + 1 independent As and Bs survive:

$$A_{\nu_2} := A_{\nu_2,1} = P_\chi (-1)^j A_{-\nu_2,-1}$$
$$\mathcal{B}_{\nu_1} := \mathcal{B}_{\nu_1,1} = P_\chi (-1)^j \mathcal{B}_{-\nu_1,-1} \qquad (6.4)$$

The full angular distribution can now be written as a sum over these (real) helicity amplitudes with the density matrices ρ for the initial and final lepton pairs and including rotations $d(\theta_{\gamma\gamma})$ after the emission of γ_1 and before the emission of γ_2 .

$$W_j(\theta_1,\varphi_1,\theta_{\gamma\gamma},\theta_2,\varphi_2) = \sum_{\substack{\mu_1,\mu_2=\pm 1 \\ \nu_1,\tilde{\nu}_1,\nu_2,\tilde{\nu}_2}} \rho^{\lambda_1,\mu_1-\tilde{\nu}_1}(\theta_1,\varphi_1)\, \mathcal{B}_{|\nu_1|}\mathcal{B}_{|\tilde{\nu}_1|}\, d^j_{-\nu_1,\nu_2}(\theta_{\gamma\gamma}) \times \qquad (6.5)$$
$$\times\, d^j_{-\tilde{\nu}_1,\tilde{\nu}_2}(\theta_{\gamma\gamma})\, A_{|\nu_2|} A_{|\tilde{\nu}_2|}\, \rho^{*-\lambda_2,\tilde{\nu}_2-\mu_2}(\theta_2,\varphi_2) \ .$$

For the five angles we adopt the conventions of ref. (22) (compare Fig. 12). These five angles are not measured in the lab system and experimentally they have to be computed from the measured angles and momenta event by event.
In the case of j = 0 (6.5) reduces to

$$W_0(\theta_1,\varphi_1,\theta_{\gamma\gamma},\theta_2,\varphi_2) \sim (1+\cos^2\theta_1)(1+\cos^2\theta_2) \qquad (6.6)$$

For j = 1,2, however, the sum of (6.5) is quite lengthy. We have used REDUCE [24] to compute the sum and yield

$$W_1(\theta_1,\varphi_1,\theta_{\gamma\gamma},\theta_2,\varphi_2) \sim (A_{11}\mathcal{B}_{11} + A_{11}\mathcal{B}_{00} + A_{00}\mathcal{B}_{11}) +$$
$$+ (A_{00}-A_{11})(\mathcal{B}_{00}-\mathcal{B}_{11})\cos^2\theta_{\gamma\gamma}$$
$$+ \tfrac{1}{2}(A_{00}-A_{11})\mathcal{B}_0\mathcal{B}_1 \cos\varphi_1 \sin 2\theta_1 \sin 2\theta_{\gamma\gamma} \qquad (6.7)$$
$$+ \tfrac{1}{2}(\mathcal{B}_{11}-\mathcal{B}_{00})A_0 A_1 \cos\varphi_2 \sin 2\theta_2 \sin 2\theta_{\gamma\gamma}$$
$$+ \tfrac{1}{2} A_0 A_1 \mathcal{B}_0 \mathcal{B}_1 \sin 2\theta_1 \sin 2\theta_2 (\sin\varphi_1 \sin\varphi_2 \cos\theta_{\gamma\gamma} + \cos\varphi_1 \cos\varphi_2 \cos 2\theta_{\gamma\gamma}),$$

$$W_2(\theta_1,\varphi_1,\theta_{\gamma\gamma},\theta_2,\varphi_2) \sim$$

$$(2A_{11}+A_{22})(2B_{11}+B_{22}) + (A_{00}+\tfrac{3}{2}A_{22})(B_{00}+\tfrac{3}{2}B_{22}) - 3A_{22}B_{22}$$

$$+ 6\cos^2\theta_{\gamma\gamma}\left[(A_{00}-\tfrac{1}{2}A_{22})(B_{00}-\tfrac{1}{2}B_{22}) - 2(A_{00}-A_{11})(B_{00}-B_{11})\right]$$

$$+ \cos^4\theta_{\gamma\gamma}\left[3(A_{00}+\tfrac{1}{2}A_{22})(B_{00}+\tfrac{1}{2}B_{22}) + 6(A_{00}-2A_{11})(B_{00}-2B_{11})\right.$$

$$\left. - 2(2A_{11}+\tfrac{1}{2}A_{22})(2B_{11}+\tfrac{1}{2}B_{22})\right]$$

$$+\sqrt{6}\cos 2\varphi_1\, B_{02}\left[\tfrac{1}{2}A_{22} - A_{00} + \tfrac{1}{\sqrt{6}}A_{02}\cos 2\varphi_2 +\right.$$

$$+ 2\cos^2\theta_{\gamma\gamma}(2A_{00}-2A_{11}-\tfrac{1}{\sqrt{6}}A_{02}\cos 2\varphi_2)$$

$$\left. + \cos^4\theta_{\gamma\gamma}(4A_{11}-3A_{00}-\tfrac{1}{2}A_{22}+\sqrt{\tfrac{3}{2}}A_{02}\cos 2\varphi_2)\right]$$

$$+\sqrt{6}\cos 2\varphi_2\, A_{02}\left[\tfrac{1}{2}B_{22} - B_{00} + \tfrac{1}{\sqrt{6}}B_{02}\cos 2\varphi_1 +\right.$$

$$+ 2\cos^2\theta_{\gamma\gamma}(2B_{00}-2B_{11}-\tfrac{1}{\sqrt{6}}B_{02}\cos 2\varphi_1)$$

$$\left. + \cos^4\theta_{\gamma\gamma}(4B_{11}-3B_{00}-\tfrac{1}{2}B_{22}+\sqrt{\tfrac{3}{2}}B_{02}\cos 2\varphi_1)\right] \qquad (6.8)$$

$$+\sqrt{6}\sin\varphi_1\sin 2\varphi_2\sin 2\theta_1 B_1 A_{02}\sin\theta_{\gamma\gamma}\left[\tfrac{1}{\sqrt{3}}B_0 - \tfrac{1}{\sqrt{2}}B_2 - \cos^2\theta_{\gamma\gamma}(\sqrt{3}B_0+\tfrac{1}{\sqrt{2}}B_2)\right]$$

$$-\sqrt{6}\sin\varphi_2\sin 2\varphi_1\sin 2\theta_2 A_1 B_{02}\sin\theta_{\gamma\gamma}\left[\tfrac{1}{\sqrt{3}}A_0 - \tfrac{1}{\sqrt{2}}A_2 - \cos^2\theta_{\gamma\gamma}(\sqrt{3}A_0+\tfrac{1}{\sqrt{2}}A_2)\right]$$

$$-2\sin 2\varphi_1\sin 2\varphi_2 A_{02}B_{02}\left[\cos\theta_{\gamma\gamma} - 3\cos^3\theta_{\gamma\gamma}\right]$$

$$+\cos\varphi_1\sin 2\theta_1\sin 2\theta_{\gamma\gamma} B_1\left[\sqrt{3}B_0(2A_{11}+\tfrac{4}{\sqrt{6}}A_{02}\cos 2\varphi_2) - \tfrac{1}{\sqrt{3}}B_0(\tfrac{3}{2}A_{22}+3A_{00}) +\right.$$

$$\left. + \tfrac{1}{\sqrt{2}}B_2(\tfrac{3}{2}A_{22}-3A_{00}) + \cos^2\theta_{\gamma\gamma}(\tfrac{1}{2}A_{22}-4A_{11}-\sqrt{6}A_{02}\cos 2\varphi_2+3A_{00})(\tfrac{1}{\sqrt{2}}B_2+\sqrt{3}B_0)\right]$$

+

$$
\begin{aligned}
&- \cos\varphi_2 \sin 2\theta_2 \sin 2\theta_{\gamma\gamma} A_1 \Big[\sqrt{3} A_0 \big(2B_{11} + \tfrac{4}{\sqrt{6}} B_{02} \cos 2\varphi_1\big) - \tfrac{1}{\sqrt{3}} A_0 \big(\tfrac{3}{2} B_{22} + 3 B_{00}\big) + \\
&+ \tfrac{1}{\sqrt{2}} A_2 \big(\tfrac{3}{2} B_{22} - 3 B_{00}\big) + \cos^2\theta_{\gamma\gamma} \big(\tfrac{1}{2} B_{22} - 4 B_{11} - \sqrt{6} B_{02} \cos 2\varphi_1 + 3 B_{00}\big)\big(\tfrac{1}{\sqrt{2}} A_2 + \sqrt{3} A_0\big)\Big] \\
&+ \sin 2\theta_1 \sin 2\theta_2 A_1 B_1 \Big[\big(\cos\varphi_1 \cos\varphi_2 - \cos\theta_{\gamma\gamma} \sin\varphi_1 \sin\varphi_2\big)\big(A_0 B_0 + \sqrt{\tfrac{3}{2}} A_0 B_2 + \sqrt{\tfrac{3}{2}} A_2 B_0 - \tfrac{3}{2} A_2 B_2\big) + \\
&+ \cos^2\theta_{\gamma\gamma} \cos\varphi_1 \cos\varphi_3 \big(\tfrac{3}{2} A_2 B_2 - \tfrac{15}{\sqrt{6}} A_2 B_0 - \tfrac{15}{\sqrt{6}} A_0 B_2 - 11 A_0 B_0\big) + \cos^3\theta_{\gamma\gamma} \times \\
&\times \big(\sin\varphi_1 \sin\varphi_3 + 4 \cos\theta_{\gamma\gamma} \cos\varphi_1 \cos\varphi_3\big)\big(\tfrac{1}{\sqrt{2}} B_2 + \sqrt{3} B_0\big)\big(\tfrac{1}{\sqrt{2}} A_2 + \sqrt{3} A_0\big)\Big] ,
\end{aligned}
$$

with

$$
\begin{aligned}
A_{11} &\equiv A_1^2 \sin^2\theta_2 & \mathcal{B}_{11} &\equiv \mathcal{B}_1^2 \sin^2\theta_1 \\
A_{00} &\equiv A_0^2 (1+\cos^2\theta_2) & \mathcal{B}_{00} &\equiv \mathcal{B}_0^2 (1+\cos^2\theta_1) \\
A_{22} &\equiv A_2^2 (1+\cos^2\theta_2) & \mathcal{B}_{22} &\equiv \mathcal{B}_2^2 (1+\cos^2\theta_1) \\
A_{02} &\equiv A_0 A_2 \sin^2\theta_2 & \mathcal{B}_{02} &\equiv \mathcal{B}_0 \mathcal{B}_2 \sin^2\theta_1
\end{aligned}
\qquad (6.9)
$$

Eq. (6.7) and (6.8) can now be specified to physical processes with explicit dynamics. A specialisation to electric dipole photon transitions e.g. is achieved by setting $A_0 = A_1$, $B_0 = B_1$ in (6.7) and $A_2 = \sqrt{2}\, A_1 = \sqrt{6}\, A_0$, $B_2 = \sqrt{2}\, B_1 = \sqrt{6}\, B_0$ in (6.8). However, the power of these formulae reaches further. To show this we start with (6.8). Here we assume the first γ^* transition to be electric dipole again, $B_2 = \sqrt{2}\, B_1 = \sqrt{6}\, B_0$. For the second transition we identify γ_2 with one gluon, V_2 with the second gluon, integrate over θ_2, φ_2 and find that we are now describing the process (3.8), $e^+e^- \longrightarrow V_1 \longrightarrow \gamma_1 + {}^3P_2 \longrightarrow \gamma_1 + q\bar{q}$. $\theta_{\gamma\gamma}$ becomes $\theta_{\gamma j}$. Specifying the dynamics to (3.6), $A_1 = A_0 = 0$, we obtain the distribution (3.9). Setting $A_2 = 0$ and $A \equiv A_1/A_0$ on the other hand leads to (3.11).

We now turn to (6.7) and again assume the first transition to be electric dipole, $B_1 = B_0$. (6.7) can now be compared to process (4.7), $e^+e^- \longrightarrow V_1 \rightarrow$ $\longrightarrow \gamma + {}^3P_1 \longrightarrow \gamma + g + q\bar{q}$, by identifying γ_2 with the gluon

g, and the μ pair with $q\bar{q}$. V_2 plays the rôle of the intermediate heavy gluon in (4.7). A transformation of the angles in coordinate system 2 (with respect to $\gamma_2 \equiv g$) by $\Theta_{\gamma g}$ to a system 2' in which $\gamma_1 \equiv \gamma$ (unobserved) is the polar axis, allows to integrate over the angles of the gluon and we obtain (4.8). There $A \equiv A_1/A_0$. Note that A_1 corresponds to a longitudinal heavy intermediate gluon and A_0 to a transversal one because of the transverse polarisations of the massless gluon g. But (4.8) is symmetric under an exchange $A_1 \longleftrightarrow A_0$.

Note further that in the process competing with (4.7) the angles are defined as discussed above for process (3.8) and therefore this process differs quite much from (4.7).

Acknowledgement.

I am indebted to M. Krammer for many helpful discussions during the course of this work. I also thank H. Joos for reading the manuscript.

References.

1) H. Fritzsch, M. Gell-Mann and H. Leutwyler, Phys. Lett. 47B (1973) 365;
D.J. Gross and F. Wilczek, Phys. Rev. D8 (1973) 3497;
S. Weinberg, Phys. Rev. Lett. 31 (1973) 494 .

2) D.J. Gross and F. Wilczek, Phys. Rev. Lett. 30 (1973) 1343;
H.D. Politzer, Phys. Rev. Lett. 30 (1973) 1346.

3) T. Appelquist and H.D. Politzer, Phys. Rev. Lett. 34 (1975) 43,
Phys. Rev. D12 (1975) 1404;
A. De Rújula and S.L. Glashow, Phys. Rev. Lett. 34 (1975) 46.

4) R. Barbieri, R. Gatto and R. Kögerler, Phys. Lett. 60B (1976) 183;
A.I. Alekseev, Soviet Phys. JETP 34 (1958) 826;
R. Barbieri, R. Gatto and E. Remiddi, Phys. Lett. 61B (1976) 465;
L.B. Okun et al., Physics Reports 41C (1978) 1.

5) J. Kuti and P. Hasenfratz, Physics Reports 40C (1978) 75 and references
therein.

6) E. Eichten et al., Phys. Rev. D11 (1978) 3090.

7) A.B. Henriques, B.H. Kellet and R.G. Moorhouse, Phys. Lett. 64B (1976) 85;
B. Billoire and A. Morel, Nucl. Phys. B135 (1978) 131;
G. Bhanot and S. Rudaz, Cornell preprint CLNS 393 (1978).

8) R.F.Schwitters et al., Phys. Rev. Lett. 35 (1975) 1320 ;
G. Hanson et al., Phys. Rev. Lett. 35 (1975) 1609 ;
G. Hanson, SLAC PUB 2118 (1978).

9) J. Ellis, M.K. Gaillard and G.G. Ross, Nucl. Phys. B111 (1976) 253.

10) K. Koller and T.F. Walsh, Phys. Lett. 72B (1977) 227 and 73B (1978) 504;
K. Koller, H. Krasemann and T.F. Walsh, DESY 78/37(1978).

11) T.A. DeGrand, Y.J. Ng and S.H.H. Tye, Phys. Rev. D16 (1977) 3251;
S.J. Brodsky, T.A. DeGrand and R.R. Horgan, Phys. Lett. 73B (1978) 203;
H. Fritzsch and K.H. Streng, Phys. Lett. 74B (1978) 90;
K. Hagiwara, Nucl. Phys. B137 (1978) 164.

12) S.W. Herb et al., Phys. Rev. Lett. 39 (1977) 252.

13) Ch. Berger et al., Phys. Lett. 76B (1978) 243;
C.W. Dardeen et al., Phys. Lett. 76B (1978) 246 , DESY 78/44 (1978);
J.K. Bienlein et al., DESY 78/45 (1978)

14) M. Krammer and H. Krasemann, Phys. Lett. 73B (1978) 58.

15) A. De Rújula et al., Nucl. Phys. B138 (1978) 387.

16) L.B. Okun et al. in Ref 4). Many conversion factors between photonic and gluonic decays are given there.

17) T. Appelquist and H.D. Politzer in ref. 3).

18) H. Krasemann, Thesis DESY T-78/01.

19) An overview over the scaling laws is given by
C. Quigg and J.L. Rosner, Fermilab PUB 77/90 THY(1977).

20) R. v. Royen and V.F. Weisskopf, Nuov. Cim. 50 (1967) 617 and 51 (1967) 583.

21) K. Gottfried, Phys. Rev. Lett. 40 (1978) 598.

22) G. Karl, S. Meshkov and J.L. Rosner, Phys. Rev. D13 (1976) 1203.

23) P.K. Kabir and A.J.G. Hey, Phys. Rev. D13 (1976) 3161;
H.B. Thacker and P. Hoyer, Nucl. Phys. B106 (1976) 147.

24) A.C. Hearn, STAN-CS-70-181(1970).

Figure Captions.

Fig. 1) The basic process for quark jets in e^+e^-.

Fig. 2) The short distance process of Fig. 1 within the colour bag of a larger volume. When the separating quarks reach the bag surface, they fragment into jets of white hadrons. Colour bleaching processes are carried by soft quarks and gluons with a wavelength comparable to the bag diameter.

Fig. 3) The 3 gluon decay of a $Q\bar{Q}$ ground state in e^+e^-. Only one permutation of this diagram is shown.

Fig. 4) Process of Fig. 3 displayed analog to Fig. 2. The decay of the $Q\bar{Q}$ state is not pointlike but hopefully covers a volume $\ll$ bag volume.

Fig. 5) The process $e^+e^- \longrightarrow V' \longrightarrow \gamma + {}^3P_j \longrightarrow \gamma + gg$.

Fig. 6) Process of Fig. 5a displayed analog to Fig. 2. The final state is a (monochromatic) γ and two hadron jets. There are two loops involving the heavy quark Q, one for the $V' = 2^3S_1$ state, one for the ${}^3P_j$ state.

Fig. 7) Three (a,b,c) next order diagrams for the decay of ${}^3P_1$ without permutations.

Fig. 8) The display of an event $e^+e^- \longrightarrow V' \longrightarrow \gamma + {}^3P_1 \longrightarrow$
$\longrightarrow \gamma + g\,g\bar{q} \longrightarrow \gamma + 2$ jets
analog to Fig. 6.

Fig. 9) Angles in process (3.8), $e^+e^- \longrightarrow V' \longrightarrow \gamma + {}^3P_2 \longrightarrow \gamma + gg \rightarrow \gamma + 2$ jets. γ defines the polar axis and the jet $\varphi = 0$. Then the angles of the beam are θ, φ in the lab system. $\theta_{\gamma j}$ is the angle between the jet and γ in the c.m.s. of the 2 jets.

Fig. 10) The squared matrix element for the ${}^3P_1 \longrightarrow gq\bar{q}$ decay.

Fig. 11) The integrand of (4.6) as a function of the (mass)^2 of the heavy gluon in arbitrary units. The wave function cutoff described in the text is shown for the charmonium and Υ system. The relative weight of the heavy gluon helicities is also shown.

Fig. 12) The three coordinate systems for
$e^+e^- \longrightarrow V' \longrightarrow \gamma_1 + {}^3P_j \longrightarrow \gamma_1 + \gamma_2 + V_2 \longrightarrow \gamma_1 + \gamma_2 + \mu^+\mu^-$
according to ref. (22).

a) in the c.m.s. of the beam (lab system). γ_1 is the polar axis. γ_2 defines $\varphi_1 = 0$, the beam (e^-, say) has the angles θ_1, φ_1.

b) $\theta_{\gamma\gamma}$ is the angle between γ_1 and γ_2 in the c.m.s. of the ${}^3P_j$ state.

c) in the c.m.s. of the μ pair. γ_2 is the polar axis, γ_1 defines $\varphi_2 = 0$, the μ pair (μ^-, say) has the angles θ_2, φ_2.

Table captions.

Table 1) The model hadronic widths of some $Q\bar{Q}$ states with $\alpha_s(3\ \text{GeV}) \simeq 0.4$.

Table 2) Estimates of some branching fractions and widths for Υ' decays, taking exp. charmonium results as input and using scaling laws described in Ch. 5.

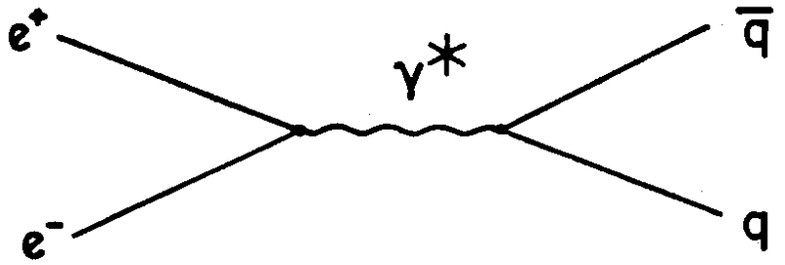
e+
e-
γ*
q̄
q

Fig. 1

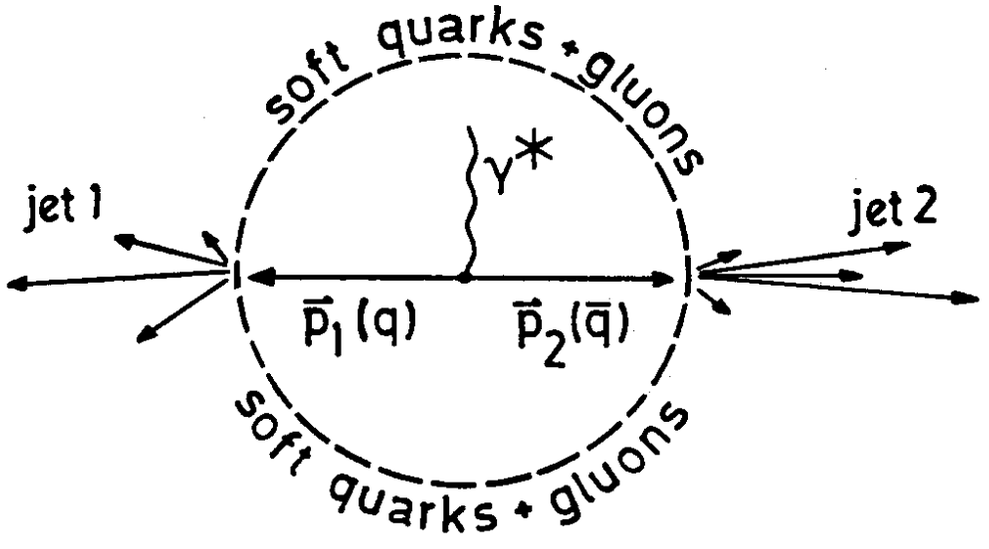
soft quarks + gluons
γ*
jet 1
jet 2
p⃗1 (q)
p⃗2 (q̄)
soft quarks + gluons

Fig. 2

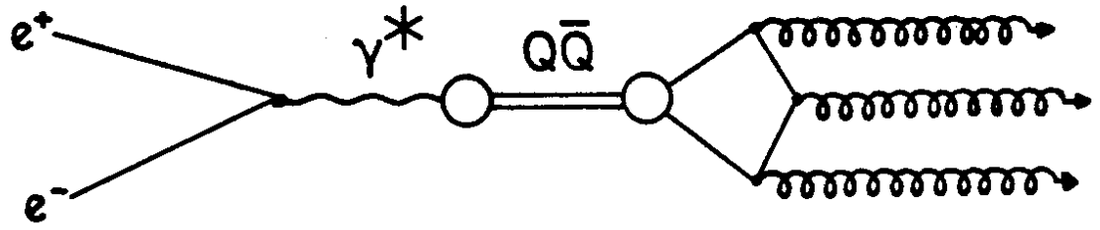
e+
e-
γ*
QQ̄

Fig.3

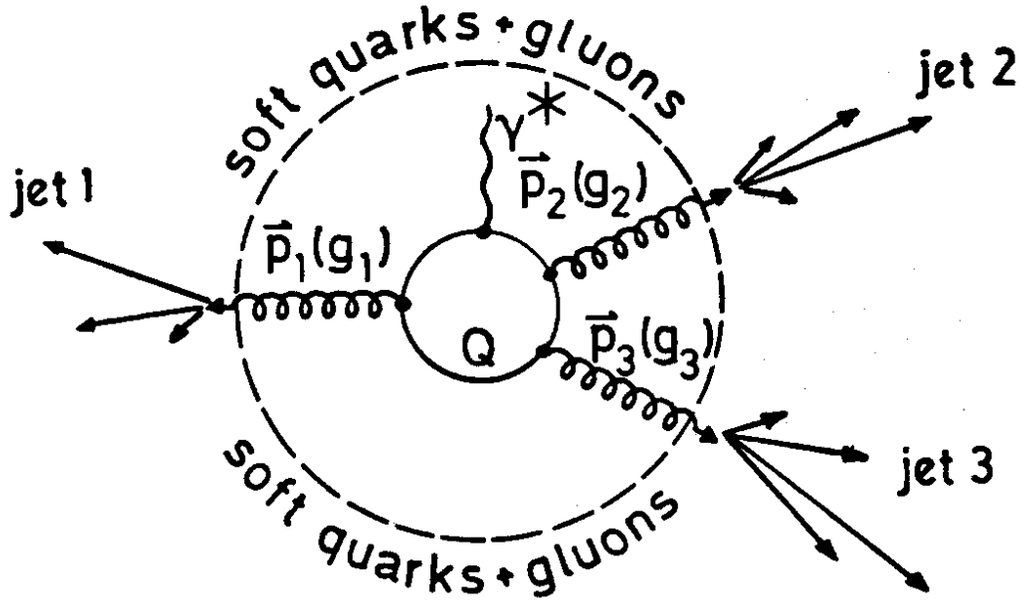
soft quarks + gluons
jet 1
jet 2
jet 3
γ*
$\vec{P}_1(g_1)$
$\vec{P}_2(g_2)$
$\vec{P}_3(g_3)$
Q
soft quarks + gluons

Fig.4

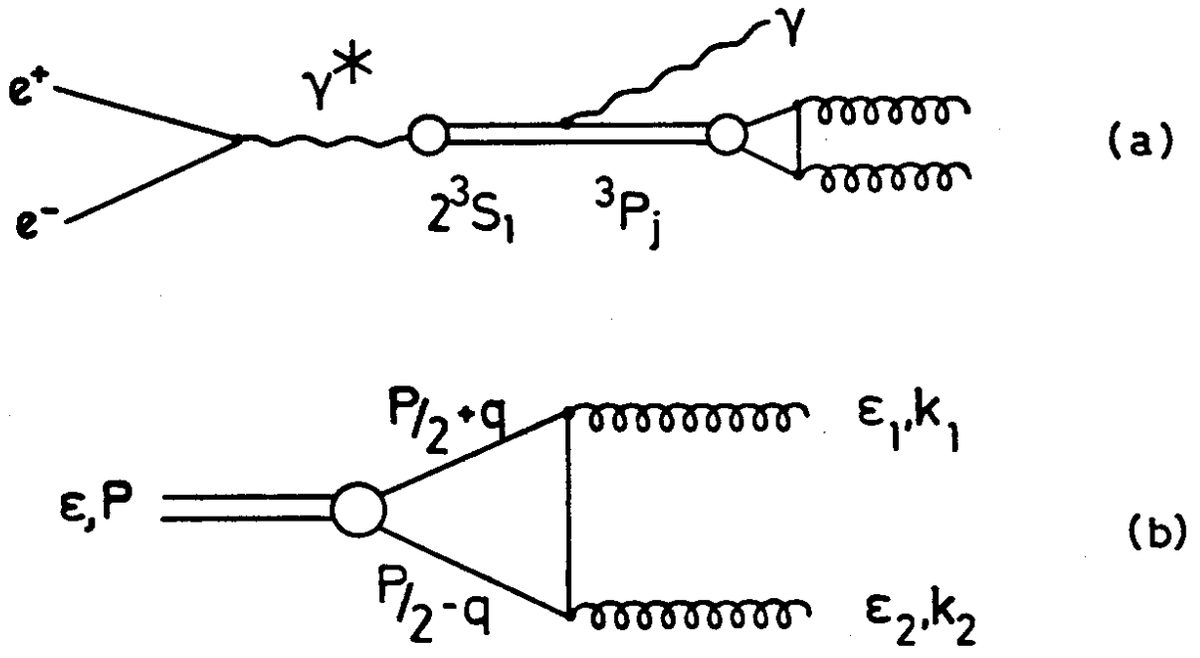

Fig.5

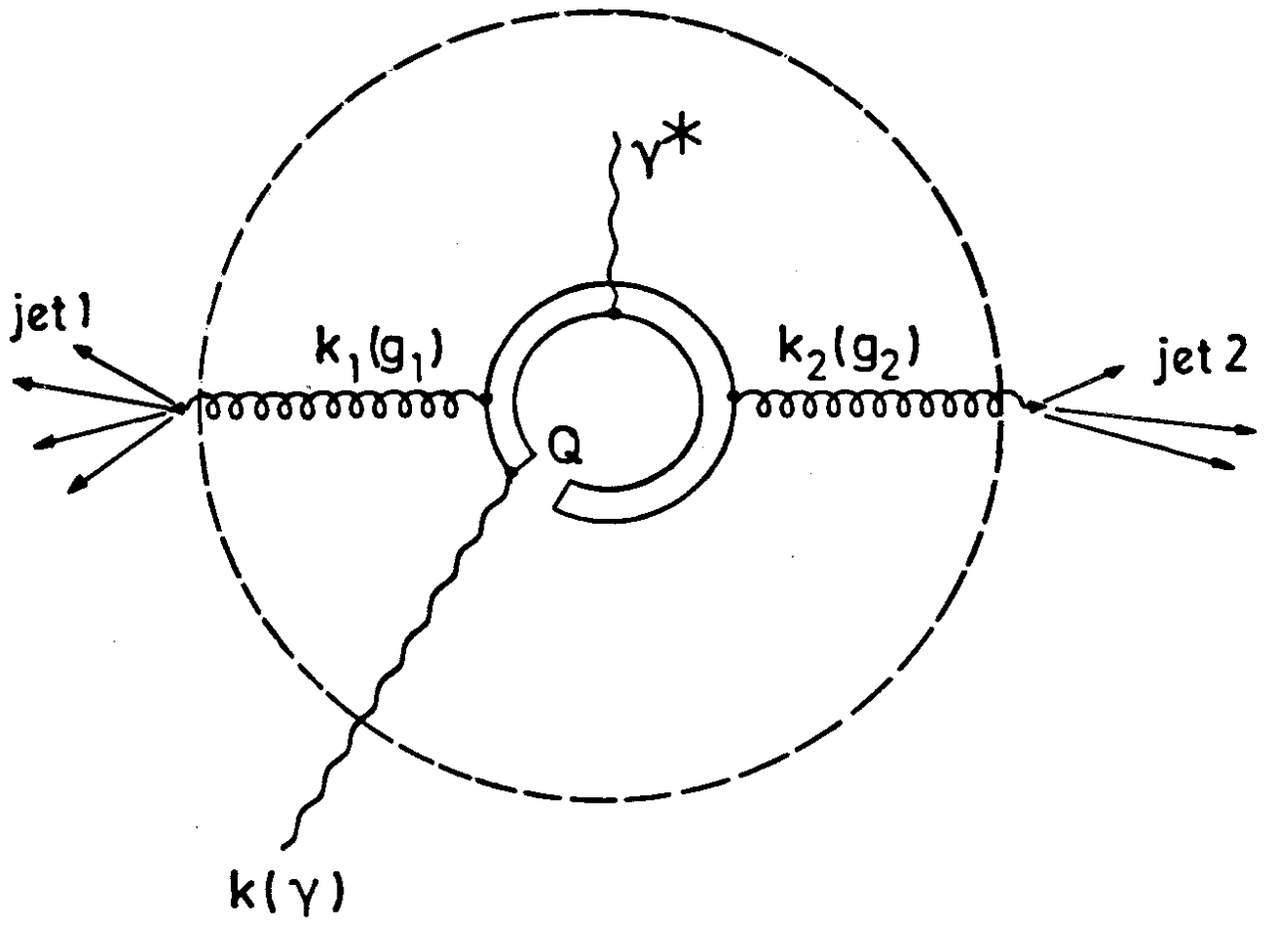

Fig. 6

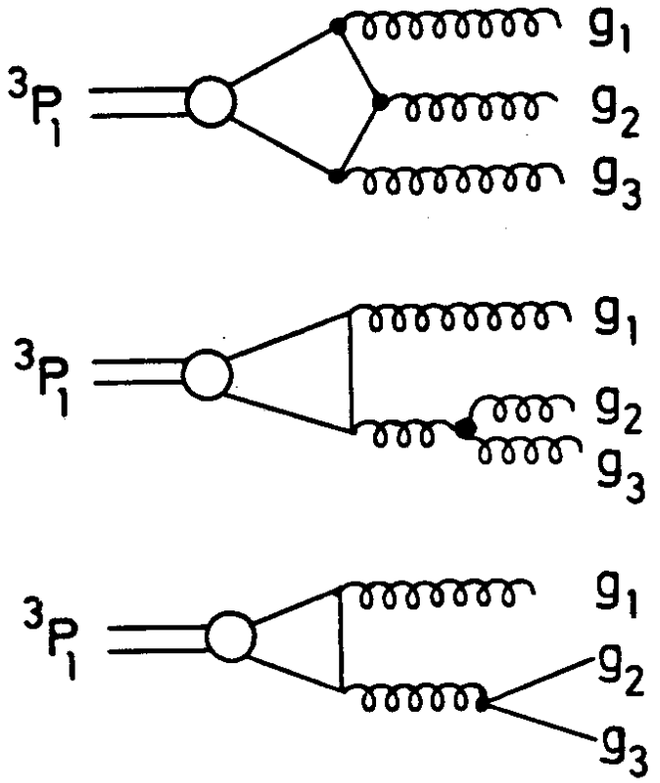
$^3P_1$
g_1
g_2
g_3
(a)
$^3P_1$
g_1
g_2
g_3
(b)
$^3P_1$
g_1
g_2
g_3
(c)

Fig.7

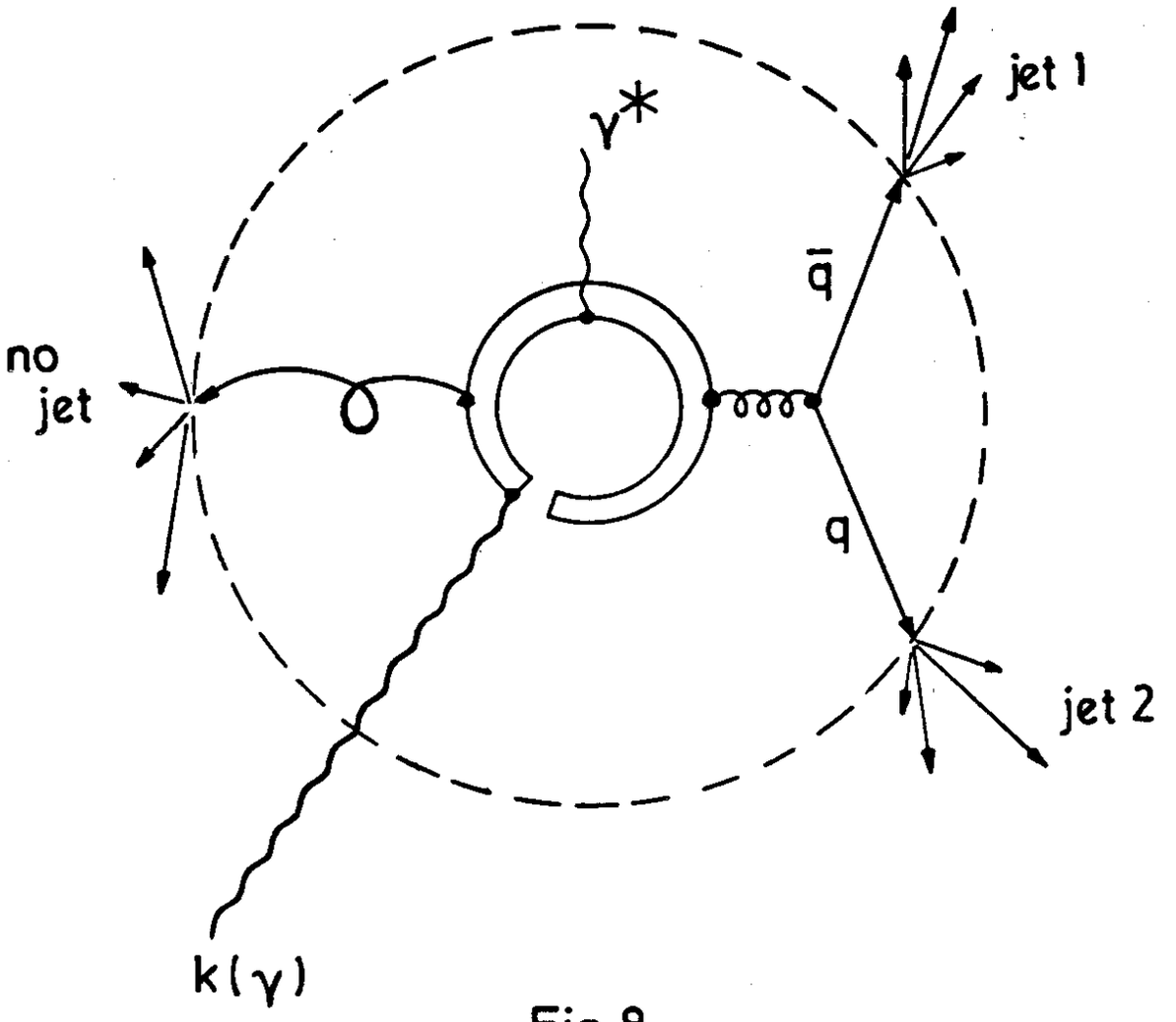
jet 1
γ^*
$\bar{q}$
no
jet
q
jet 2
k(γ)

Fig. 8

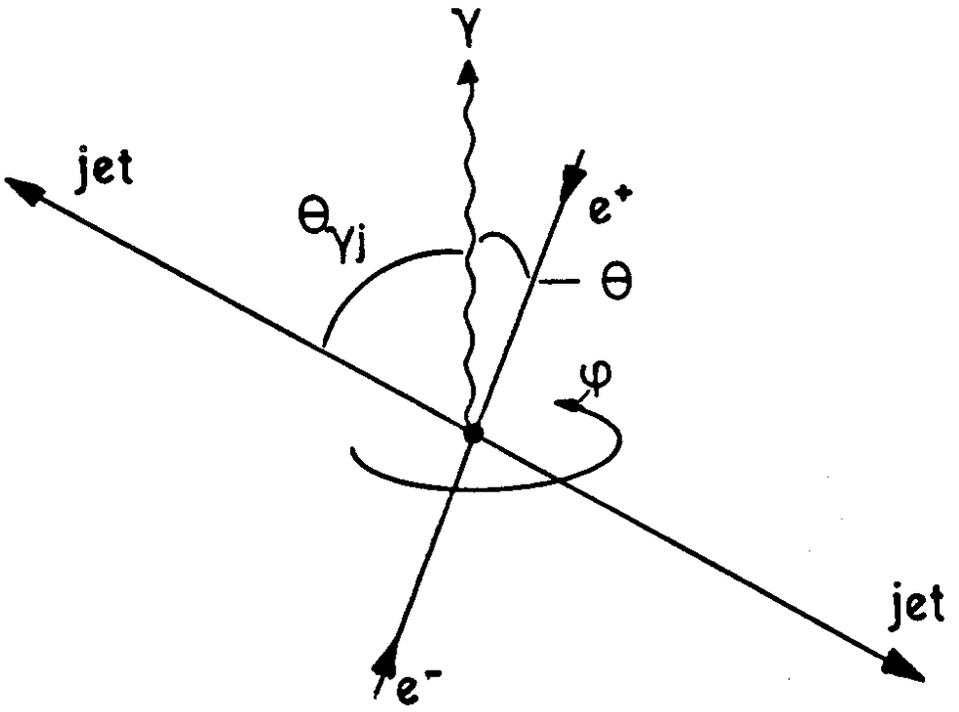

Fig. 9

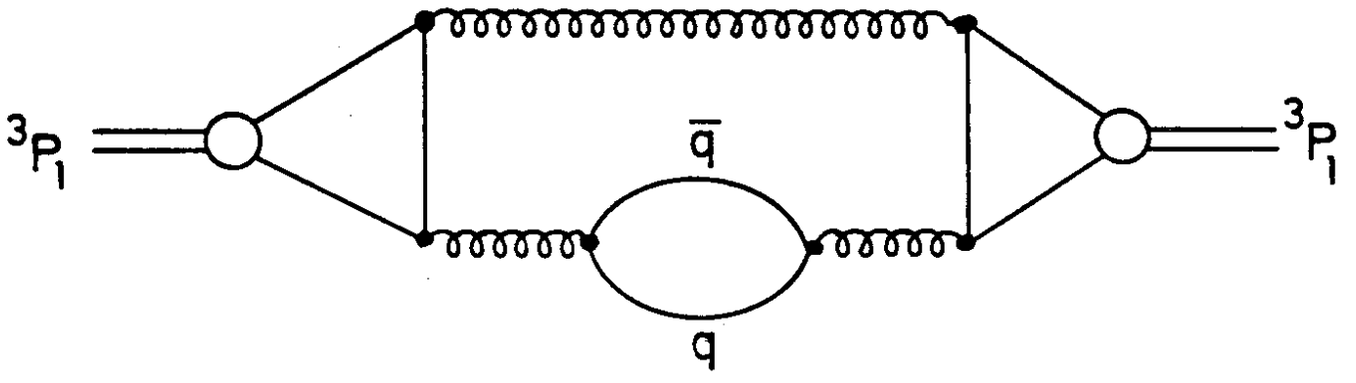

Fig. 10

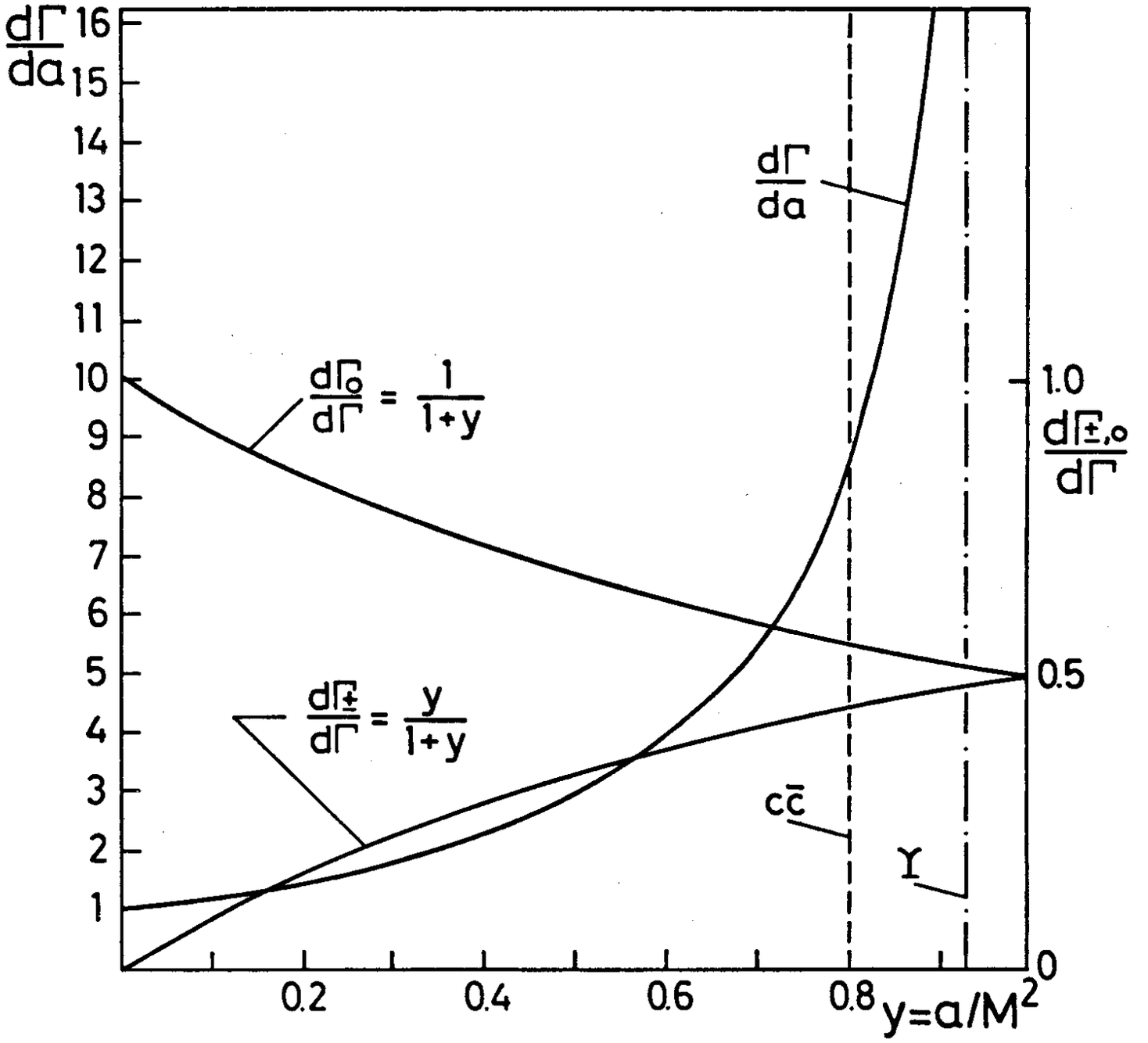
dΓ/da
16
15
14
13
12
11
10
9
8
7
6
5
4
3
2
1
dΓ/da
dΓ₀/dΓ = 1/(1+y)
dΓ±/dΓ = y/(1+y)
cc̄
ϒ
1.0
dΓ±,₀/dΓ
0.5
0
0.2
0.4
0.6
0.8
y=a/M²

Fig. 11

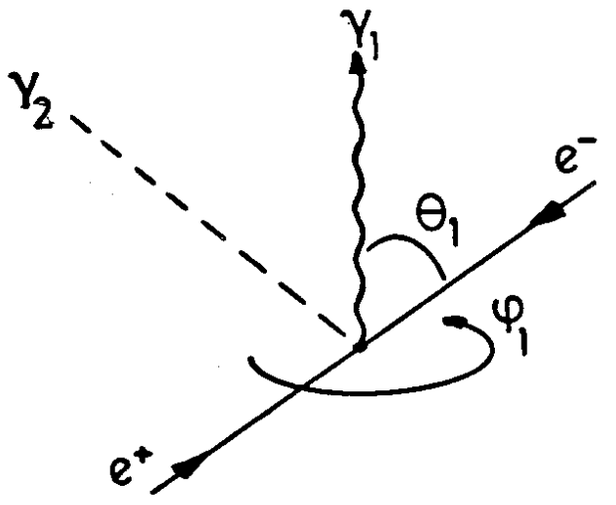

(a)

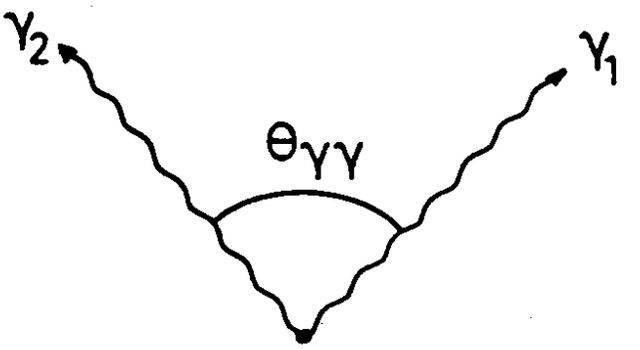

(b)

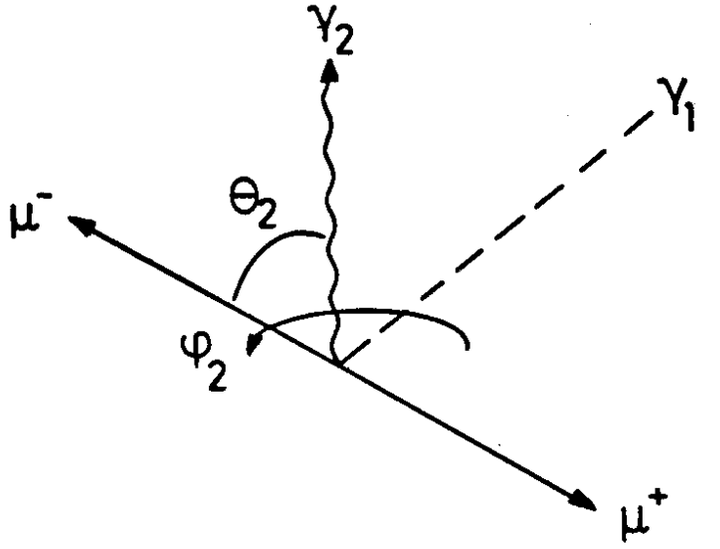

(c)

Fig. 12

J^{PC}	0^{-+}	0^{++}	1^{++}	2^{++}
$\Gamma_{hadr}(c\bar{c})$ [MeV]	20	11	0.7	3
$\Gamma_{hadr}(b\bar{b})$	9	1	0.1	0.25

Table 1

$\psi'(3.7)$ partial widths Input [keV]		scaling law	$\Upsilon'(10)$ partial widths [B.R.] $e_b = -1/3\, e$ [keV]
e^+e^-	1.9	e_Q^2	0.47 [1.7%]
"γ^*"			3.2 [0.11]
$^3P_2 + \gamma$	15		1.5 [5.5%]
$^3P_1 + \gamma$	15	$e_Q^2 k^3 m_Q^{-1}$	1.1 [4%]
$^3P_0 + \gamma$	15.5		0.6 [2%]
$3g$	20	α_s^3	10 [0.36]
$\pi\pi\, ^3S_1$	105	m_Q^{-2}	11 [0.4]
		$\Gamma(\Upsilon') \approx 28$ keV	

$^3P_j(c\bar{c})$ B.R. Input [%]			scaling law	$^3P_j(\Upsilon)$ B.R. [%] $e_b = -1/3\, e$		
$j=0$	$j=1$	$j=2$		$j=0$	$j=1$	$j=2$
$^3S_1 + \gamma$ 3	35	14	$e_Q^2 k^3 m_Q^{-1}$	4	29	10
$2g$ 97	65	86	$\alpha_s^2 m_Q^{-1}$	96	71	90
Branching fraction $\Upsilon' \to \gamma + 2$ jets [%]				2	3	5

Table 2